Research Square

Preprints are preliminary reports that have not undergone peer review.
They should not be considered conclusive, used to inform clinical practice,
or referenced by the media as validated information.

Increased water availability accelerates C cycling in a dry forest ecosystem

Luisa I. Minich

luisa.minich@gmail.com

Swiss Federal Institute for Forest, Snow and Landscape Research WSL, Switzerland
https://orcid.org/0000-0002-4874-8590

Claudia Guidi

Swiss Federal Institute for Forest, Snow and Landscape Research WSL, Switzerland

Alois Zürcher

Swiss Federal Institute for Forest, Snow and Landscape Research WSL, Switzerland

Dylan Geissbühler

Laboratory for the Analysis of Radiocarbon with AMS, Department of Chemistry, Biochemistry and Pharmaceutical Sciences, University of Bern, Switzerland

Margaux Moreno Duborgel

Swiss Federal Institute for Forest, Snow and Landscape Research WSL, Switzerland

Katrin Di Bella Meusburger

Swiss Federal Institute for Forest, Snow and Landscape Research WSL, Switzerland

Negar Haghipour

Laboratory for Ion Beam Physics, Department of Physics, ETH Zurich, Switzerland

Jonas Gisler

Swiss Federal Institute for Forest, Snow and Landscape Research WSL, Switzerland

Marcus Schaub

Swiss Federal Institute for Forest, Snow and Landscape Research WSL, Switzerland

Lukas Wacker

Laboratory for Ion Beam Physics, Department of Physics, ETH Zurich, Switzerland

Philip Gautschi

Laboratory for Ion Beam Physics, Department of Physics, ETH Zurich, Switzerland

Frank Hagedorn

Swiss Federal Institute for Forest, Snow and Landscape Research WSL, Switzerland

---

Research Article

Keywords: Carbon cycling, drought, irrigation, radiocarbon, soil respiration, heterotrophic respiration, autotrophic respiration, source contribution

Posted Date: January 21st, 2026

DOI: https://doi.org/10.21203/rs.3.rs-8649982/v1

License: This work is licensed under a Creative Commons Attribution 4.0 International License. Read Full License

Additional Declarations: The authors declare no competing interests.

Abstract

Climate change is intensifying the frequency and severity of droughts, with profound implications for carbon (C) cycling in forest ecosystems. While progress has been made in understanding how drought alters plant and microbial ecophysiology, it remains unclear how these changes affect the overall magnitude and pace of C cycling within the plant-soil continuum.

In this study, we examined the effects of 22 years of experimental irrigation in a naturally drought-prone Scots pine forest. We integrated long-term measurements of C inputs (i.e., litterfall) and outputs (i.e., soil respiration) with radiocarbon (^{14}C) analysis of soil organic carbon, fine roots, and CO_2 from *in situ* soil respiration and its autotrophic and heterotrophic components.

Our study demonstrates that long-term shifts in water availability enhance both C inputs and outputs, reshaping C cycling within the plant-soil system. Radiocarbon (^{14}C) analysis revealed that irrigation accelerated C cycling within plants and the organic layer, reducing the time that assimilated C remained in the ecosystem before being respired back to the atmosphere. The observed increase in soil respiration under irrigation was largely driven by enhanced autotrophic activity, associated with greater fine root biomass. Concurrently, the decomposition of labile, young organic matter intensified under irrigation, potentially contributing to a net C loss from the organic layer. Despite this increased respiration under irrigation, ^{14}C contents in bulk SOC indicated greater inputs of young C to the mineral soil and enhanced downward translocation of C from the organic layer to the mineral phase, possibly through rhizodeposition and soil faunal activity. The enhanced input to the mineral soil under irrigation results in net C gains and may promote C stabilization through organo-mineral interactions and aggregate formation. Our findings also indicate that drought conditions limit both the magnitude and rate of C cycling within the plant-soil continuum and potentially reduce long-term C sequestration in mineral soils.

Introduction

Climate change is projected to increase the intensity and frequency of drought events (IPCC, 2021), with consequences for carbon (C) cycling in forest ecosystems and in their soils (Gao et al., 2021; Guidi et al., 2022; Schindlbacher et al., 2012). By constraining the metabolic activity of both plants and soil microbes, drought impacts multiple components of the C cycle, reducing both C inputs and outputs. Drought decreases net primary productivity (Ciais et al., 2005; Zhou et al., 2016), reduces allocation of assimilated C to the soil (Fuchslueger et al., 2016; Joseph et al., 2020), and alters fine root biomass and production (Brunner et al., 2019; Xu, 2023). Additionally, drought can reduce the activity and diversity of soil fauna, further disrupting belowground activity and processes (Guidi et al., 2022; Kudureti et al., 2023). Consequently, drought suppresses C outputs from soils with reduced soil respiration (e.g., Apostolakis et al., 2023; Xu, 2023). Drought affects the major sources of soil respiration: autotrophic respiration that includes all respiratory processes within the rhizosphere (Trumbore, 2006) and which is linked to plant C allocation and metabolism (Gao et al., 2021; Hagedorn et al., 2016), and heterotrophic respiration, which involves the mineralization of soil organic matter (SOM) by microorganisms

(Trumbore, 2006). The contribution of autotrophic respiration to total soil respiration is directly affected by drought through reduced allocation and metabolization of assimilates in the rhizosphere (Gao et al., 2024; Hagedorn et al., 2016) and indirectly through changes in fine root biomass (Apostolakis et al., 2023). Limited water availability also impacts heterotrophic respiration by suppressing microbial activity (Guidi et al., 2022; Schimel, 2018). While it is well known that drought reduces soil respiration in forest ecosystems (e.g., Apostolakis et al., 2023; Schindlbacher et al., 2012; Xu, 2023), it remains uncertain whether this decline is primarily driven by autotrophic (e.g., Hinko-Najera et al., 2015; Huang et al., 2018) or heterotrophic respiration (Borken et al., 2006; Zheng et al., 2021).

Drought-induced changes in C inputs and outputs lead to a redistribution of C among different pools in forest ecosystems (Bose et al., 2022; Guidi et al., 2022; Rog et al., 2024) and to changes in the rate at which C is transferred between these pools (Gao et al., 2021). Long-term irrigation of a forest ecosystem naturally exposed to drought initially increased aboveground biomass, followed by a shift toward greater belowground biomass allocation (Bose et al., 2022). Here, drought reduced and delayed the transfer of recently assimilated C from aboveground plant tissues to the rhizosphere (Gao et al., 2021; Joseph et al., 2020). Responses may be ecosystem specific and depend on the magnitude of drought (Solly et al., 2023), e.g. with Norway spruce maintaining high root exudation under drought (Brunn et al., 2022). Drought conditions may suppress litter decomposition (Santonja et al., 2017; Schindlbacher et al., 2012) and limit the transfer of soil organic carbon (SOC) from the organic layer to the mineral soil through reduced soil fauna activity (Guidi et al., 2022). As a result, SOC accumulates in the organic layer, while mineral SOC stocks are lower than under higher water availability (Guidi et al., 2022). Despite advances in understanding drought effects on C inputs and outputs (e.g., Apostolakis et al., 2023; Bose et al., 2022; Xu, 2023), the extent to which these shifts alter the scale and rate of C cycling, and consequently long-term C storage, within the plant-soil continuum remains poorly understood.

The radioactive C isotope (^{14}C) is a powerful tool to investigate C cycling in ecosystems, as it provides insights into the age of C in various pools, informing about the time C has spent in the ecosystem since photosynthesis (Trumbore, 2009). Nuclear weapons testing in the mid-20th century caused a sharp increase in atmospheric $^{14}CO_2$ levels – commonly referred to as the “bomb-spike” – which nearly doubled natural background levels in the Northern Hemisphere. Since then, atmospheric $^{14}CO_2$ concentrations have declined enabling researchers to trace C incorporation and cycling across ecosystem compartments on decadal time scales (Graven et al., 2024). When combined with stable C isotope (^{13}C) analysis, ^{14}C measurements of respired CO_2 from *in situ* soil respiration and its autotrophic and heterotrophic sources offer a robust, non-destructive method to assess not only the age of respired C, but also source contributions to total soil respiration (e.g., Borken et al., 2006; Schuur & Trumbore, 2006). Radiocarbon analysis has previously been applied in short-term throughfall exclusion experiments to assess the effects of drought on autotrophic and heterotrophic respiration (e.g., Borken et al., 2006; Muhr & Borken, 2009; Schindlbacher et al., 2012). While such studies offer insights into the short-term responses of plant metabolic processes and microbial activity to changes in water availability, their ability to capture long-term effects on soil C cycling is limited (Bose et al., 2022).

In this study, we aimed to investigate long-term effects of irrigation on C cycling in a naturally dry Scots pine forest ecosystem. We conducted our study in a large-scale irrigation experiment established in 2003 in a Scots pine forest located in one of the driest inner-alpine regions of the European Alps. The forest in this area is naturally exposed to prolonged and repeated summer droughts, which have intensified in recent decades due to climate warming and the associated increase in water loss through evapotranspiration (Hunziker et al., 2022; Rigling et al., 2013). The long-term release from natural drought stress through irrigation provides an ideal set-up to investigate C cycling in the plant-soil continuum under persistent and repeated drought, and to compare it with non-water-limited conditions. Here, we combined long-term measurements of soil C inputs (i.e., litterfall) and outputs (i.e., soil respiration) with measurements of belowground ecosystem traits (i.e., fine root biomass), SOC properties (i.e., SOC stocks, C mineralization), and ^{14}C analysis in bulk SOC, fine roots, and respired CO_2 from *in situ* soil respiration and from its autotrophic and heterotrophic components. This approach allowed us to identify structural shifts in the ecosystem induced by long-term changes in water availability and to evaluate their effects on soil C cycling. We aimed to understand (i) how long-term irrigation affects the magnitude and pathways of C inputs (i.e. litterfall, fine roots) and outputs (i.e. soil respiration and its autotrophic and heterotrophic sources), (ii) if and how irrigation changes the age of C in different compartments of the ecosystem, and (iii) how changes in water availability influence C stabilization in the soil.

Materials and methods

Pfynwald – long-term irrigation experiment

The study site is located in a Scots pine (*Pinus sylvestris*) forest with sporadic occurrences of pubescent oak (*Quercus pubescens*) situated in the Rhone Valley (46° 18' N, 7° 36' E, 615 m a.s.l., Valais, Switzerland). The region is one of the driest inner-alpine valleys of the European Alps, characterized by a mean annual precipitation (MAP) of 576 mm and a mean annual temperature (MAT) of 10.6°C (data from MeteoSwiss station Sion; Bose et al., 2022). The study was conducted within the long-term irrigation experiment in the Pfyn forest established in 2003 to investigate the effects of natural drought on ecosystem traits and functions (Bose et al., 2022; Hunziker et al., 2022). The soil is classified as a shallow Pararendzina developed on an alluvial fan (Gao et al., 2021). The experimental setup consists of 8 plots (25 x 40 m), each separated by a buffer zone of 5 m (Herzog et al., 2014). Four plots were randomly assigned to an irrigation treatment, while the remaining four serve as naturally dry controls, referred to as “irrigation” and “dry control”, respectively. Irrigation is applied via a sprinkler system during nights from May to October, supplying an additional amount of 600 mm water annually (~ 5 mm per night). The irrigation water is taken from an adjacent but hydrologically disconnected water channel fed by the Rhone River (Bose et al., 2022).

Soil and root sampling and processing

Soil and roots were sampled in November 2019 after the end of the irrigation period. Four soil pits were excavated with a 20 × 20 cm frame in each plot. Soil sampling and processing are described in Guidi et al., 2022. The organic layer (OL) was separated in the field into litter (Oi) and partially decomposed, humified material (Oe/Oa). Afterwards, the mineral soil was excavated by depth increments (0–2, 2–5, 5–10, 10–20 cm). In the laboratory, the field-moist organic layer and mineral soil samples were hand-homogenized by sieving at 4 mm with stones and roots sorted out. Roots separated from soil sieving were carefully rinsed over a 1-mm sieve with tap water. Fine roots (diameter ≤ 2 mm) were hand-picked and visually separated into Scots pine roots and roots from other species. Fine roots were freeze-dried and weighed. The four subsamples per plot were then pooled into one composite sample per plot and depth increment. In each of the two plots (one irrigated, and one dry control) where *in situ* CO_2 was sampled for ^{14}C analysis, one additional soil pit was excavated in 2023 and samples were used for soil incubations (see paragraph: *"CO_2 sampling from soil and root incubations"*). For this, mineral soil samples were collected at depth intervals of 0–5, 5–10, and 10–20 cm, while the organic layer was sampled separately into Oi and Oe/Oa horizons.

C mineralization

Potential C mineralization was measured from samples collected in 2011 as described in Hartmann et al., 2017. Soil samples were incubated in 300 cm^3 glass jars at 20°C and adjusted to 50% water holding capacity. The amount of soil used varied based on SOC content, ranging from 7 g to 90 g dry weight per sample. Respiration rates were measured immediately after water addition and subsequently once per week over a 28-day period, using a flow-through system connected to a LI-COR gas analyser (LI-8100A, LI-COR INC., Lincoln, NE, USA).

Long-term measurements of soil respiration and litterfall

Since 2012, *in situ* soil respiration has been measured on a monthly basis on 32 locations across the experimental site (four replicates per plot). Measurements were less frequent during winter months (December–February) due to snow cover and low temperatures. Soil CO_2 efflux was measured on permanently installed PVC collars (Ø = 20 cm) inserted 2–4 cm into the soil. For the measurements, we used custom-made static flux chambers equipped with diffusion-based infrared gas analyser (IRGAs) and relative humidity/temperature sensors (GMP343 CO_2 probe, HMP75 rH/T probe; Vaisala, Vantaa, Finland), correcting CO_2 measurements for water vapour content. The increase in CO_2 concentration within the chamber headspace was recorded over a 5-minute interval. Respiration rates were calculated as the linear rate of CO_2 accumulation over time, corrected for atmospheric pressure and mean chamber temperature based on the ideal gas law (Butterbach-Bahl et al., 2011). Measured soil CO_2 flux with the Vaisala system were validated regularly against a LI-8100A soil CO_2 flux system with a LI 8100 – 102 survey chamber (LI-COR INC., Lincoln, NE, USA). Simultaneously to soil respiration measurements, soil temperature was recorded at a depth of 5–10 cm. To assess gravimetric water content (GWC), soil

samples were collected near the collars during each measurement campaign and oven-dried at 105°C for 48 hours. Annual respiration rates were calculated by summing up monthly mean soil respiration rates. Annual litterfall has been monitored since 2016. Litter was collected once or twice a year (December and/or April) from four locations within each plot using rectangular samplers (0.25 m^2) placed on the forest floor. Collected samples were dried at 40°C for 72h.

CO sampling of in situ soil respiration

Soil-respired CO_2 was sampled at single time points in August 2023 and March 2024 from two plots, representing each treatment. In August, CO_2 was collected from one location per plot, whereas in March, samples were taken from three different locations per plot to account for spatial variability. For gas sampling, three cylindrical PVC chambers (Ø = 30 cm; height = 15–25 cm; volume ~ 15 L) were inserted 3–5 cm into the soil surface at a distance of 1–2 m from each other to capture spatial variability in soil respiration. Chambers were installed 1–2 weeks prior to sampling to allow CO_2 fluxes to stabilize following potential installation-induced disturbance. Prior to gas sampling, respiration rates were monitored over a 5- to 10-minute interval using a LI-COR gas analyser (LI-8100A, LI-COR INC., Lincoln, NE, USA). Thereafter, chambers were flushed with CO_2-free air five times the chamber volume and sealed until CO_2 levels reached ~ 1000 ppm for subsequent ^{14}C analysis. After flushing the chambers, the gas samples were collected using a flow-through system connected to the LI-COR gas analyser. Two H_2O traps within the flow-through system prevented moisture from entering the LI-COR pump and samplng bag during the measurement and sample collection. First, all gas tubes and H_2O traps were scrubbed with a CO_2 scrubber (soda lime) to remove atmospheric background CO_2 in the flow-through system. Air from the three chambers was composited into a 2 L sampling bag (Cali-5-Bond, Calibrated Instruments, LLC, USA). For this, one-third of the bag was sequentially filled from each chamber by connecting the flow-through system and isolating the chambers with valves after each fill. To avoid pressure imbalances during sampling, all three chambers were interconnected via gas tubing, allowing for pressure equilibration across headspaces. For ^{13}C analysis, gas was sampled from each of the three chambers separately, transferring headspace air into pre-evacuated 12 mL Exetainer® vials using a 60 mL syringe. Soil temperature was monitored before and after the CO_2 sampling. Soil samples were collected from 0–5 cm soil depth for the determination of GWC.

CO_2 sampling from soil and root incubations

Isotopic signatures of autotrophic and heterotrophic endmembers were determined via short-term root and soil incubations. Root incubations were prepared *in situ* during the sampling campaigns. Fine roots (< 2 mm), including mycorrhizae, were excavated from 0–10 cm depth within the chambers immediately after gas sampling. After carefully removing soil particles and rinsing the roots in ultrapure water, samples from all three chambers were pooled and incubated promptly to minimize isotopic shifts post-excision (Midwood et al., 2006). Approximately 10 g of fresh roots were placed into 2 L glass bottles

wrapped in aluminum foil to exclude light, flushed with CO_2-free air, and incubated overnight at ~ 22°C. Gas was collected the next day into a 2 L sampling bag using a flow-through system similar as described for *in situ* CO_2 sampling. If the CO_2 concentration inside the bottle was high enough for ^{14}C analysis (> 2000 ppm), we pumped the air from the bottle through a 2 L air bag, which was pre-filled with CO_2-free air, to maintain the pressure inside the flow-through system. The sampling was completed when the air from the bottle and 2 L air bag was thoroughly mixed within the system (i.e., CO_2 concentration remained constant). $\delta^{13}C$ of root respiration was sampled in the same way as for *in situ* soil respiration. Soil incubations followed the same procedure and were conducted for each depth layer, resulting in one heterotrophic $\Delta^{14}CO_2$ value per treatment and depth. Depending on SOC content and layer, 10–140 g dry-equivalent soil was incubated at 22°C and field moisture. Incubation duration ranged from one to seven days, depending on respiration rates. Basal respiration was calculated over the full incubation period and weighted by dry mass per depth.

Isotopic analysis of bulk soil samples

Radiocarbon (^{14}C) was analysed in soil (all depths) and root (5–10 cm depth) samples excavated in 2019. Inorganic C was removed from all samples through fumigation with 37% HCl (Komada et al., 2008; Walthert et al., 2010). Samples were acidified at 60°C for 72 hours and subsequently neutralized using NaOH pellets under the same conditions. Prior to use, all glassware was pre-combusted at 550°C for 5 hours to eliminate potential contaminants. ^{14}C measurements of SOC in bulk soil were conducted using a MIni radioCArbon DAting System (MICADAS, ETH Zurich, Switzerland; Synal et al., 2007) equipped with a gas ion source and coupled to an Elemental Analyzer (EA vario MICRO cube, Elementar, Germany; Ruff et al., 2007) at the Laboratory of Ion Beam Physics, ETH Zurich. Measurement uncertainties ranged from 6 to 8‰.

Isotopic analysis of CO samples

The $^{13}CO_2$ content of all gas samples was measured using an isotope-ratio mass spectrometer (IRMS Gas-Bench II coupled with a Delta-V Advanced IRMS, Thermo GmbH, Germany) at the Swiss Federal Research Institute of Forest, Snow and Landscape WSL. For ^{14}C analysis, gas samples were graphitized using an Air Loading Facility (ALF; Gautschi, 2017) coupled to an Automated Graphitization Equipment (AGE3, ETH Zurich, Switzerland; Wacker, Němec, et al., 2010) with an integrated zeolite trap to adsorb CO_2 from the sampling bag. The $^{14}CO_2$ content of all gas samples were measured using a MICADAS (ETH Zurich, Switzerland) or a Low Energy AMS (LEA, ETH Zurich & IonPlus AG, Switzerland; Ramsperger et al., 2024). Measurement uncertainties were < 2‰. For data evaluation, the standard Oxalic Acid II (Mann, 1983) and blank material from the ^{14}C-free phthalic anhydride (PhA) were measured alongside the samples and evaluated with the BATS software (Wacker, Christl, et al., 2010). Graphitization and ^{14}C measurements were performed at the Laboratory of Ion Beam Physics, ETH Zurich, Switzerland. In

samples from 10–20 cm soil depth, $\delta^{13}CO_2$ values were less depleted than $\delta^{13}C$ values of bulk SOC, suggesting a potential contribution of carbonate weathering to the soil-emitted CO_2. To estimate the potential contribution of this process, we applied a two-endmember mass balance model, assuming a $\delta^{13}C$ of 0‰ for carbonate and $\delta^{13}CO_2$ = $\delta^{13}C$-SOC. The estimated contribution of carbonate weathering to soil respiration and its isotopic signatures was minimal (< 1–2%), consistent with findings from other forest sites (e.g., Schindlbacher et al., 2012). Also, their contribution would not affect the share of autotrophic respiration and therefore would not affect our result interpretation.

Source partitioning of soil respiration

Soil-respired CO_2 collected *in situ* from the chamber headspace was partitioned into autotrophic, heterotrophic, and residual atmospheric sources using Bayesian mixing models. Source apportionment was performed with the MixSIAR package (R version 3.1.12; Moore & Semmens, 2008; Stock et al., 2018) and with a custom implementation in Python. A detailed description of the approach is presented in Minich et al., 2025. For source partitioning in March, we used heterotrophic $\Delta^{14}CO_2$ values from incubated soil samples collected in August.

Statistical analysis

Linear mixed-effect models (LME) were fitted to investigate the effect of treatment and soil depths on $\Delta^{14}C$ values of heterotrophically respired CO_2 and SOC in bulk soil, as well as on SOC stocks, fine root biomass, and C mineralization with plots included as random effects (R package lmerTest, version 3.1.3; Kuznetsova et al., 2017) to account for spatial heterogeneity. Transformations of the response variables were conducted in case the assumption of normal distribution (tested with Shapiro-Wilk normality test) or homoscedasticity (tested with Levene's test and plots of fitted vs. residuals) was violated. Analysis of variance (ANOVA) was conducted on the fixed effects (treatment, depth) of the models to assess their significance and interaction. Following the main effects, post hoc pairwise comparisons were conducted using estimated marginal means (EMMs) (R package emmeans, version 1.10.4; Lenth, 2024) to assess significant differences between treatment within each depth and vice versa, adjusted for multiple comparisons using Tukey's method. Generalized least square models (GLS) were fitted to investigate the effect of treatment on long-term soil respiration rates, soil moisture, and soil temperature (R package nlme, version 3.1.166; Pinheiro et al., 2025). The model included seasonal cycling terms – sin(2π x month / 12) and cos(2π x month / 12) – to capture intra-annual variation in the soil respiration, temperature, and moisture. An interaction term between treatment and these seasonal predictors was included to assess whether seasonal responses differed across treatments. To account for temporal autocorrelation a first-order autoregressive structure was specified within each year. The response variables were log-transformed to meet model assumptions regarding normality and homoscedasticity of residuals. ANOVA was performed on the fixed effects (treatment, seasonality terms) to assess their significance. We further fitted a GLS to investigate how soil temperature and moisture affected soil respiration under dry control and irrigated conditions. The seasonal cycling terms were excluded as the seasonal variation is already reflected in soil temperature and moisture. Interaction terms between all

predictor variables (soil temperature, soil moisture, treatment) allowed us to assess whether relationships between environmental drivers and respiration rates varied between treatments.

Results

Long-term irrigation effects on soil respiration

Long-term measurements revealed that irrigation significantly increased soil respiration (SR; $p < 0.001$; Table S2), by ~ 66% on an annual basis with an overall mean respiration rate of 111 ± 64 mg CO_2-C m^{-2} h^{-1} in dry control and 185 ± 111 mg CO_2-C m^{-2} h^{-1} in irrigation plots (averaged across 2012–2024; Table S1). The increase in SR in the irrigation treatment was most pronounced during the irrigation period (May-October) (+ 79%; $p < 0.001$; Fig. 1b, Table S1, Table S2). Although not significant, SR increased by 18% in the non-irrigation period (November-April) (Fig. 1b, Table S1). While the increase of SR under irrigation relative to the dry control treatment (i.e., drought effect: $SR_{dry\ control}$ / $SR_{irrigation}$) exhibited seasonal variation with lower values in summer than in winter, there was no trend across the entire period between 2012 and 2024 (Figure S2). However, soil respiration in the dry control closely corresponded to precipitation during the irrigation period, reducing the apparent drought effect in years with higher precipitation (Fig. 1, Figure S2). The relationship between the drought effect and soil moisture in the dry control treatment was well described by a Boltzmann fit, showing that SR in the dry control remained lower than in the irrigation treatment even at soil moisture levels above 35% (w-% of moist soil; Fig. 2b).

While soil moisture significantly differed between treatments during the irrigation period ($p < 0.001$, Figure S1, Table S2), soil temperature was almost identical in dry control and irrigated plots (Figure S1, Table S2). In the irrigation treatment, soil temperature had a significant effect ($p = 0.020$, Table S3) on respiration rates which increased exponentially with increasing temperature (Fig. 2a). In the dry control treatment, soil moisture was the main driving factor of respiration rates ($p = 0.003$, Table S3), while the effect of soil temperature was not significant ($p = 0.23$, Fig. 2a). The interaction between soil temperature and soil moisture was highly significant in the dry control treatment ($p < 0.001$), but less pronounced under irrigation ($p = 0.015$, Table S3). Irrigation significantly increased the effect of soil temperature on soil respiration ($p = 0.010$, Table S3, Fig. 2a).

Long-term irrigation effects on source contribution

$\Delta^{14}CO_2$ values of *in situ* soil respiration were consistently lower in the irrigation (August: 1‰, March: -5‰) compared to the dry control treatment (August: 19‰, March: 4‰) in both seasons (Figure S4). The difference between treatments was more pronounced in August than in March. Overall, *in situ* $\Delta^{14}CO_2$ values were lower in March than in August but exceeded the atmospheric background levels measured in both months (March: +32‰; August: − 14‰).

$\Delta^{14}CO_2$ values of autotrophic respiration were slightly lower (August: -12‰, March: -16‰) and thus closer to atmospheric $\Delta^{14}CO_2$ in the irrigation treatment than in the dry control treatment (August: -8‰, March: -13‰). Although $\Delta^{14}CO_2$ values of heterotrophic respiration were slightly higher in the irrigation treatment (mean across the soil profile: 18‰) than in the dry control treatment (mean across the soil profile: 12‰; Table 1, Figure S4), this difference was not significant (Table S4, Table S5).

Overall, source partitioning showed that the relative contribution of heterotrophic respiration was higher in August than in March (Fig. 3a). Heterotrophic respiration dominated total soil respiration in the dry control, with relative contributions of 86% in August and 58% in March. In the irrigated soils, autotrophic and heterotrophic respiration contributed equally to total soil respiration in August, while autotrophic respiration accounted for 64% in March (Fig. 3). While absolute heterotrophic respiration from the mineral soil was similar between treatments, respired CO_2 originating from the organic layer and autotrophic sources was higher from irrigated soils. During August, these two sources respired 10 to 13 times more CO_2 in irrigated soils compared to the dry control (Fig. 3b, Figure S3).

Long-term irrigation effects on C inputs, SOC distribution, and C mineralization

Both aboveground (i.e., litterfall) and belowground (i.e., fine root biomass) C inputs increased under irrigation. On average across the years 2016–2023, litterfall increased by 49% from 333 ± 47 g m^{-2} yr^{-1} in the dry control treatment to 496 ± 98 g m^{-2} yr^{-1} under irrigation. Total fine root biomass (Scots pine + other species in OL + 0–20 cm soil depth) increased by 25% under irrigation, with mean values rising from 285 g m^{-2} in the dry control to 356 g m^{-2} in the irrigation treatment (Table 1, Fig. 4). While fine root biomass increased significantly in the mineral soil under irrigation (+ 44%; Table S4), especially at 2–5 cm (+ 78%) and 5–10 cm depth (+ 72%), it was reduced in the organic layer (-66%; Fig. 4), also considering the reduced organic layer mass compared to the dry control (– 36%; Guidi et al., 2022). In the organic layer, SOC stocks decreased by 1.0 kg m^{-2}, whereas in the mineral soil, SOC stocks increased by 0.8 kg m^{-2}.

Cumulative C mineralization across the soil profile measured upon one month incubation at 20°C was 44% higher in the irrigation treatment (45.1 ± 8.1 mg CO_2–C g SOC^{-1} $month^{-1}$) compared to the dry control treatment (65.0 ± 18.7 mg CO_2–C g SOC^{-1} $month^{-1}$; Fig. 4). This higher C mineralization was most pronounced in the organic layer and upper 0–2 cm of the mineral soil (Fig. 4, Table 4.1, Table S5).

Table 1
Mean values of SOC stocks, fine root biomass, C mineralization, $\Delta^{14}C$ values of bulk SOC and heterotrophically respired CO_2 across soil depth profiles under dry control and irrigated conditions.

	Soil depth	SOC stock	Fine root biomass	C mineralization	$\Delta^{14}C$-SOC	$\Delta^{14}CO_2$
	cm	kg m^{-2}	g m^{-2}	mg CO_2-C g SOC^{-1} $month^{-1}$	‰	‰
Dry control	Oi	0.42 ± 0.12		71.1 ± 18.6	35.2 ± 26.2	-13.0
	Oe/Oa	1.21 ± 0.67	48.1 ± 33.7	28.9 ± 7.3	86.6 ± 29.7	-2.9
	0–2	1.17 ± 0.15	85.2 ± 26.7	28.9 ± 10.7	107.6 ± 19.4	27.0
	2–5	0.94 ± 0.23	58.6 ± 16.4	51.7 ± 4.9	98.2 ± 23.8	
	5–10	0.85 ± 0.25	47.9 ± 15.8	68.3 ± 4.1	83.2 ± 19.0	27.6
	10–20	1.04 ± 0.26	44.7 ± 14.1	46.9 ± 8.1	69.1 ± 23.6	19.5
	Profile	5.6	285	45	80	12
Irrigation	Oi	0.31 ± 0.09		90.1 ± 27.9	28.2 ± 8.4	-0.3
	Oe/Oa	0.30 ± 0.26	16.5 ± 15.9	54.8 ± 10.2	41.6 ± 11.4	1.6
	0–2	1.09 ± 0.21	98.8 ± 7.7	55.7 ± 18.2	80.1 ± 25.5	38.9
	2–5	1.26 ± 0.24	104.5 ± 19.8	62.8 ± 24.9	107.5 ± 31.6	
	5–10	1.18 ± 0.14	81.9 ± 18.7	77.4 ± 13.0	86.7 ± 12.9	31.6
	10–20	1.26 ± 0.17	54.6 ± 13.0	59.7 ± 18.1	72.5 ± 14.7	18.2
	Profile	5.4	356	65	69	18

Radiocarbon contents in SOC, respired CO_2, and fine roots

$\Delta^{14}C$-SOC values mirrored the depth-dependent differences in SOC stocks between the two treatments. In the organic layer and 0–2 cm of the mineral soil, mean $\Delta^{14}C$-SOC values were significantly lower under irrigation compared to the dry control (~ 50‰ vs. ~76‰; $p_{FH} < 0.0001$, $p_{0-2} = 0.098$; Table S5). At

greater depths (2–20 cm), this pattern reversed, with slightly higher Δ¹⁴C-SOC values in the irrigation treatment than in the dry control (~ 89‰ vs. ~84‰), although this difference was statistically not significant. Mean Δ¹⁴C values of fine roots were lower and closer to atmospheric $^{14}CO_2$ levels in 2019 in the irrigation treatment (Scots pine: 37 ± 14‰, other species: 38 ± 14‰) than in the dry control treatment (Scots pine: 48 ± 25‰, other species: 46 ± 14‰). Compared with the decline in atmospheric $^{14}CO_2$, this corresponds to ages of 9 and 11 years, respectively.

Discussion

Our study showed that long-term irrigation in a dry pine forest led to a fundamental change in C cycling in the plant-soil continuum, increasing the in- and outputs, altering the $\Delta^{14}C$ values of belowground C pools and fluxes, and thus changing the time that C spends in the ecosystem. Although irrigation enhanced the redistribution of SOC stocks and $\Delta^{14}C$ values from the organic layer to the mineral soil, effects on total SOC stocks remained negligible after 22 treatment years.

Long-term increases and shifting sources of soil respiration under irrigation

Annual soil respiration was increased by 66% in the irrigation treatment, indicating that irrigation removed the moisture limitation of respiratory processes. This is also reflected in the tight positive relationship between soil respiration and soil temperature in the irrigation treatment, while soil moisture was the main regulating factor in dry control conditions (Table S3). However, soil respiration in the irrigation treatment was not only enhanced during the irrigation period – when soil moisture differences were most pronounced – but also during non-irrigated periods in winter, despite similar moisture levels in both treatments (Fig. 1b, Fig. 2). This suggests that in addition to immediate plant and microbial responses to soil moisture, ecosystem adaptation must have contributed to the increased respiration rates in the irrigation treatment. In the following, we will discuss three ecosystem adaptations which likely affected responses of soil respiration to irrigation: (i) increased belowground carbon allocation by plants, (ii) increased root growth due to elevated plant water demand, and (iii) increased decomposition in the organic layer.

Our analysis of Δ¹⁴C values of *in situ* soil respiration and its sources revealed that the observed increase in total soil respiration in the irrigation treatment is primarily driven by increased autotrophic respiration as well as increased heterotrophic respiration in the organic layer (Fig. 3). We attribute higher autotrophic contributions in the irrigation treatment mainly to significant increases in fine root biomass (Fig. 4), enhancing autotrophic respiration (e.g., Apostolakis et al., 2023; Liu et al., 2016e & Buchmann, 2005; Zhang et al., 2021). Additionally, both faster and significantly enhanced allocation of newly assimilated C from plants to the rhizosphere (Gao et al., 2021; Hartmann et al., 2017; Joseph et al., 2020) likely contributed to higher autotrophic respiration under irrigation. In a ¹³C pulse-labelling study conducted in this forest, Gao et al., 2021 observed that irrigation resulted in a three- to four-fold increase

in the amount of C assimilates transferred to and respired from the soil, relative to the smaller increase observed in total soil respiration – suggesting that irrigation disproportionately enhanced autotrophic processes. This aligns with findings of reduced allocation and metabolization of recent C assimilates under dry conditions in grasslands and young beech forests, which reduced autotrophic respiration more strongly than total soil respiration (Fuchslueger et al., 2014; Hagedorn et al., 2016).

The magnitude of the increase in soil respiration in the irrigation treatment compared to dry control conditions varied with the amount of summer precipitation but generally remained relatively stable between 2012 and 2024 (Fig. 1, Figure S2). This suggests that most structural changes in the ecosystem which were responsible for the increase in soil respiration must have occurred during the initial decade of the experiment (2003–2012), prior to the beginning of continuous soil respiration measurements. Bose et al., 2022 reported that trees initially responded to increased water availability in irrigated plots with increased aboveground growth, evidenced by wider tree rings and expanded crown areas. While the enhancement in aboveground growth remained constant (Bose et al., 2022) and was even followed by a slight regression to pre-irrigation growth rates of individual trees (Vitali et al., 2024), it likely induced a greater water demand (Zweifel et al., 2020). This may have triggered a shift toward belowground biomass allocation (Poorter & Nagel, 2000), which is supported by the observed continuous increase in Scots pine fine root biomass from the start of the experiment in 2003 through 2016 (Brunner et al., 2019) and in 2019 measured here (Fig. 4). The irrigation effect on fine root biomass became not significant before 2012. One reason for the retarded belowground response could be the slow fine root growth, evidenced by the $\Delta^{14}C$-derived fine root ages of several years (Fig. 4). Taken together, we propose that both the higher contribution of autotrophic respiration as well as consistently higher total soil respiration rates in the irrigation treatment reflect a long-term adjustment in belowground biomass driven by sustained water availability and demand.

In addition to enhanced autotrophic respiration, the increase in soil respiration in the irrigation treatment was also driven by accelerated heterotrophic respiration in the organic layer, which contributed to as much as 60% to total heterotrophic respiration in irrigated soils and showed a 10-fold higher rate than dry soils in August (Fig. 3). The pronounced sensitivity of the organic layer to both drought and irrigation likely reflects its high reactivity to changes in soil moisture, its disconnection from the underlying mineral soil (Keith et al., 2010), its high content of labile SOM, and its role as a hotspot of biological activity (Schindlbacher et al., 2010). Additionally, Hartmann et al., 2017 observed a shift from oligotrophic to copiotrophic microbial life strategies under irrigation in our experiment. While oligotrophic life strategies are dominant in soils of low C availability, copiotrophic organisms dominate in soils with higher net C mineralization rate (Fierer et al., 2007). This shift might have enhanced microbial C use efficiency and microbial turnover rates (Fierer et al., 2007), thereby contributing to the observed increases in C mineralization (Fig. 4) and respiration from the organic layer (Fig. 3). The increase in both autotrophic and heterotrophic respiration from the organic layer under irrigation was more pronounced in August than in March (Fig. 3). In March, similar soil temperature and moisture conditions between treatments likely led to more comparable respiration rates and source contributions.

The small effect sizes of heterotrophic respiration in the mineral soil could be explained by long-term decreases of the irrigation effect on soil water contents, due to the greater water uptake by the larger trees (Herzog et al., 2014; Shakas et al., 2025). This effect is so pronounced that in spring, before the onset of the irrigation period, soil water potentials in irrigated treatment were even lower than in the control plots (Shakas et al., 2024). In contrast, heterotrophic respiration from the minerals soil remained largely unaffected by irrigation (Fig. 3). This is in line with previous studies, observing that reductions in heterotrophic respiration under drought are primarily related to decreased decomposition activity in the organic layer (Borken et al., 2006; Cisneros-Dozal et al., 2007; Huang et al., 2018; Schindlbacher et al., 2012).

Autotrophic contributions to total soil respiration were generally higher in March than in August which is unexpected as autotrophic respiration in forest ecosystems typically peaks during the summer months (Borken et al., 2006; Schindlbacher et al., 2012). Since autotrophic respiration is more strongly influenced by plant phenology than by soil temperature (Atarashi-Andoh et al., 2012) it seems likely that measurements in March coincided with an already active phenological phase. Additionally, air temperatures exceeded soil temperatures by up to 9.5°C during *in situ* CO_2 sampling. While low soil temperatures of 9°C likely suppressed heterotrophic microbial activity, the evergreen pine trees might have been metabolically active in the warmer air (Ferrari et al., 2018), resulting in a relatively greater proportion of autotrophic respiration during the measurement.

Irrigation-induced C losses in the organic layer and gains in the mineral soil

In addition to the shifted soil CO_2 fluxes, long-term irrigation led to a SOC redistribution in the soil profile, with decreasing SOC stocks in the organic layer but gains in the mineral soil, with minimal net effect on total SOC stocks (Fig. 4; Guidi et al., 2022). The altered SOC depth distribution by irrigation is paralleled by lower $\Delta^{14}C$ values in the organic layer and higher values in the mineral soil. Multiple mechanisms may contribute to this redistribution at higher soil moisture conditions, including an accelerated decomposition, an increased rhizodeposition (Gao et al., 2021), and an enhanced translocation and incorporation of litter materials into the mineral soils (Guidi et al., 2022). The $\Delta^{14}C$-SOC depth pattern followed historical atmospheric $\Delta^{14}CO_2$ trends, and differences in the pattern between treatments thereby allow to infer on the importance of redistribution mechanisms (Fig. 4). $\Delta^{14}C$ values were closest to recent atmospheric levels in the organic layer, peaked in 0–5 cm depth (reflecting the bomb-spike with decadal old C), followed by a decline with further depth, indicating an increasing presence of older, pre-bomb C in deeper mineral layers. $\Delta^{14}C$-SOC values closer to atmospheric levels in the organic layer and 0–2 cm depth of irrigated soils indicate a faster SOC cycling and a higher input of younger litter- and root-derived inputs compared to the dry control soil. As SOC stocks in the organic layer decreased under irrigation (Fig. 4), the acceleration of decomposition must have been stronger than the enhancement of litter inputs. A possible underlying mechanism is that irrigation enhanced the activity of the soil fauna, which is particularly drought-sensitive and transforms the organic layer (Guidi et al., 2022). In the mineral

soil below 2 cm depth, Δ^{14}C-SOC values were higher in the irrigation treatment as compared to the control treatment, indicating higher inputs of decadal old, bomb-derived C.

This pattern strongly indicates that increased SOC stocks in the mineral soil of the irrigation treatment were not caused by increased belowground plant inputs (in which case one would expect lower Δ^{14}C-SOC values). Instead, this pattern suggests increased downward translocation of bomb-derived C from the organic layer and upper mineral soil (0–2 cm) to deeper soil layers. One main vector appears to be faunal-mediated transfer and incorporation of litter and organic layer into the mineral soil (Guidi et al., 2022). Higher water availability was found to increase the abundance, composition and diversity of micro-, meso-, and macro-fauna (e.g. Guidi et al., 2022; Kudureti et al., 2023; Singh et al., 2019; Tan et al., 2021), which promotes both litter decomposition and C translocation to the mineral soil (G. Angst et al., 2024). Enhanced DOC leaching under irrigation might additionally increase C transfer from the surface layers to the mineral soil. However, this contribution is likely minor as indicated by low DOC fluxes of 13 to 26 g DOC m^{-2} yr^{-1} observed in Swiss forests with shallow organic layers and comparable mean annual precipitation (Graf Pannatier et al., 2012). Lastly, the interpretation that increased vertical translocation of organic material was the dominant mechanism behind the irrigation-induced shifts in SOC stocks is further supported by shifts in stable isotope values. In the mineral soil under irrigation, ^{13}C and ^{15}N values resembled the less processed SOC from the organic layer more closely as compared to the dry control soils (Guidi et al., 2022).

Translocation of C from surface soil layers, together with increased C inputs to the mineral phase through increased litter and rhizodeposition likely promote SOC sequestration and stabilization in deeper soil layers of the mineral soil in the irrigation treatment. Although Δ^{14}C-SOC values indicate that SOC is younger under irrigation, increased C inputs likely increase the persistence of SOC through several processes. The translocation of C into deeper soil layers likely increases the potential of this translocated C to become stabilized through mineral protection as the sorption capacity for organo-mineral associations increases with soil depth (Ahrens et al., 2020). In addition, the shift from oligotrophic to copiotrophic microbial life strategies under irrigation (Hartmann et al., 2017) and subsequent enhanced turnover of microbial biomass (Gao et al., 2021) might increase the formation of microbial products that can be stabilized through organo-mineral associations (Cotrufo et al., 2015). Furthermore, litter ingestion of soil fauna, especially earthworms, promote the occlusion of SOM in soil aggregates, which leads to the physical protection of POM and MAOM from decomposition (e.g., G. Angst et al., 2024; Š. Angst et al., 2017; Bossuyt et al., 2004).

Conclusion

Our study shows that long-term changes in soil moisture regimes enhanced both C inputs as well as outputs and reshaped C cycling within the plant-soil system, primarily driven by structural changes in the forest ecosystem. We found that irrigation increased soil respiration and accelerated C cycling within the plant system and organic layer, shortening the time that C spent in the system from C assimilation through photosynthesis until it was respired back to the atmosphere. This is primarily driven by

increased autotrophic respiration, resulting from higher fine root biomass and belowground C allocation under irrigation. Additionally, ^{14}C data revealed an accelerated SOC turnover in the organic layer and uppermost mineral soil. However, while a larger proportion of C is quickly released back to the atmosphere without entering the mineral soil, vertical changes of SOC stock and $\Delta^{14}C$ values document a SOC redistribution under irrigation. Possibly, this results from the combined effects of greater rhizosphere inputs and translocation from upper soil layers through soil faunal activity. The enhanced translocation of C to the mineral soil resulted in a net SOC gain in the soil from 0–20 cm depth, which potentially promotes C stabilization. Taken together, our findings indicate that current drought conditions limit both the magnitude and pace of C cycling within the plant-soil continuum, and potentially hinder long-term C sequestration in mineral soils.

Declarations

Acknowledgements

This study is based on data from the long-term experimental research platform Pfynwald, part of the Swiss Forest Lab and the eLTER research infrastructures. We are especially grateful to the Pfynwald core team for their support and for providing access to the research infrastructure. We also thank Petra d'Orico and Fluppi Sutter for sharing aerial images and site maps of the experimental area, and MeteoSwiss for supplying essential climate data. We gratefully acknowledge Michael Guggenbühl, Stefan Tobler, Clara Juliette Gund, Jan Ziegler, Logan James Banner, Thomas Laemmel, and Mathias Mayer for their valuable assistance during fieldwork. Our thanks also go to Daniel Christen, Daniel Wasner, Roger Köchli, and Marco Walser for their dedicated help with laboratory work. We further appreciate the expertise of André Albrecht and Urs Ramsperger in sample preparation and ^{14}C measurements, as well as the support of Alessandro Schlumpf and Ursula Graf with ^{13}C analyses. This research was funded by the Radiocarbon Inventories of Switzerland project (Grant No. 193770) of the Swiss National Science Foundation. We also gratefully acknowledge the Marie Curie funding program for supporting the PostDoc position of Claudia Guidi, whose data contributed to this study.

References

1. Ahrens B, Guggenberger G, Rethemeyer J, John S, Marschner B, Heinze S, Angst G, Mueller CW, Kögel-Knabner I, Leuschner C, Hertel D, Bachmann J, Reichstein M, Schrumpf M (2020) Combination of energy limitation and sorption capacity explains 14C depth gradients. Soil Biol Biochem 148:107912. https://doi.org/10.1016/j.soilbio.2020.107912
2. Angst G, Potapov A, Joly F-X, Angst Š, Frouz J, Ganault P, Eisenhauer N (2024) Conceptualizing soil fauna effects on labile and stabilized soil organic matter. Nat Commun 15(1):5005. https://doi.org/10.1038/s41467-024-49240-x
3. Angst Š, Mueller CW, Cajthaml T, Angst G, Lhotáková Z, Bartuška M, Špaldoňová A, Frouz J (2017) Stabilization of soil organic matter by earthworms is connected with physical protection rather than

with chemical changes of organic matter. Geoderma 289:29–35. https://doi.org/10.1016/j.geoderma.2016.11.017

4. Apostolakis A, Schöning I, Michalzik B, Ammer C, Schall P, Hänsel F, Nauss T, Trumbore S, Schrumpf M (2023) Forest Structure and Fine Root Biomass Influence Soil CO2 Efflux in Temperate Forests under Drought. Forests 14(2):411. https://doi.org/10.3390/f14020411
5. Atarashi-Andoh M, Koarashi J, Ishizuka S, Hirai K (2012) Seasonal patterns and control factors of CO2 effluxes from surface litter, soil organic carbon, and root-derived carbon estimated using radiocarbon signatures. Agric For Meteorol 152:149–158. https://doi.org/10.1016/j.agrformet.2011.09.015
6. Borken W, Savage K, Davidson EA, Trumbore SE (2006) Effects of experimental drought on soil respiration and radiocarbon efflux from a temperate forest soil. Glob Change Biol 12(2):177–193. https://doi.org/10.1111/j.1365-2486.2005.001058.x
7. Bose AK, Rigling A, Gessler A, Hagedorn F, Brunner I, Feichtinger L, Bigler C, Egli S, Etzold S, Gossner MM, Guidi C, Lévesque M, Meusburger K, Peter M, Saurer M, Scherrer D, Schleppi P, Schönbeck L, Vogel ME, Schaub M (2022) Lessons learned from a long-term irrigation experiment in a dry Scots pine forest: Impacts on traits and functioning. Ecol Monogr 92(2):e1507. https://doi.org/10.1002/ecm.1507
8. Bossuyt H, Six J, Hendrix PF (2004) Rapid incorporation of carbon from fresh residues into newly formed stable microaggregates within earthworm casts. Eur J Soil Sci 55(2):393–399. https://doi.org/10.1111/j.1351-0754.2004.00603.x
9. Brunn M, Hafner BD, Zwetsloot MJ, Weikl F, Pritsch K, Hikino K, Ruehr NK, Sayer EJ, Bauerle TL (2022) Carbon allocation to root exudates is maintained in mature temperate tree species under drought. New Phytol 235(3):965–977. https://doi.org/10.1111/nph.18157
10. Brunner I, Herzog C, Galiano L, Gessler A (2019) Plasticity of Fine-Root Traits Under Long-Term Irrigation of a Water-Limited Scots Pine Forest. Front Plant Sci 10:701. https://doi.org/10.3389/fpls.2019.00701
11. Butterbach-Bahl K, Kiese R, Liu C (2011) Measurements of Biosphere–Atmosphere Exchange of CH4 in Terrestrial Ecosystems. In *Methods in Enzymology* (Vol. 495, pp. 271–287). Elsevier. https://doi.org/10.1016/B978-0-12-386905-0.00018-8
12. Ciais P, Reichstein M, Viovy N, Granier A, Ogée J, Allard V, Aubinet M, Buchmann N, Bernhofer C, Carrara A, Chevallier F, De Noblet N, Friend AD, Friedlingstein P, Grünwald T, Heinesch B, Keronen P, Knohl A, Krinner G, Valentini R (2005) Europe-wide reduction in primary productivity caused by the heat and drought in 2003. Nature 437(7058):529–533. https://doi.org/10.1038/nature03972
13. Cisneros-Dozal LM, Trumbore SE, Hanson PJ (2007) Effect of moisture on leaf litter decomposition and its contribution to soil respiration in a temperate forest. J Geophys Research: Biogeosciences 112(G1):2006JG000197. https://doi.org/10.1029/2006JG000197
14. Cotrufo MF, Soong JL, Horton AJ, Campbell EE, Haddix ML, Wall DH, Parton WJ (2015) Formation of soil organic matter via biochemical and physical pathways of litter mass loss. Nat Geosci

8(10):776–779. https://doi.org/10.1038/ngeo2520

15. Ferrari A, Hagedorn F, Niklaus PA (2018) Disentangling effects of air and soil temperature on C allocation in cold environments: A^{14} C pulse-labelling study with two plant species. Ecol Evol 8(16):7778–7789. https://doi.org/10.1002/ece3.4215
16. Fierer N, Bradford MA, Jackson RB (2007) TOWARD AN ECOLOGICAL CLASSIFICATION OF SOIL BACTERIA. Ecology 88(6):1354–1364. https://doi.org/10.1890/05-1839
17. Fuchslueger L, Bahn M, Fritz K, Hasibeder R, Richter A (2014) Experimental drought reduces the transfer of recently fixed plant carbon to soil microbes and alters the bacterial community composition in a mountain meadow. New Phytol 201(3):916–927. https://doi.org/10.1111/nph.12569
18. Fuchslueger L, Bahn M, Hasibeder R, Kienzl S, Fritz K, Schmitt M, Watzka M, Richter A (2016) Drought history affects grassland plant and microbial carbon turnover during and after a subsequent drought event. J Ecol 104(5):1453–1465. https://doi.org/10.1111/1365-2745.12593
19. Gao D, Joseph J, Werner RA, Brunner I, Zürcher A, Hug C, Wang A, Zhao C, Bai E, Meusburger K, Gessler A, Hagedorn F (2021) Drought alters the carbon footprint of trees in soils—Tracking the spatio-temporal fate of^{13} C-labelled assimilates in the soil of an old-growth pine forest. Glob Change Biol 27(11):2491–2506. https://doi.org/10.1111/gcb.15557
20. Gao D, Luster J, Zürcher A, Arend M, Bai E, Gessler A, Rigling A, Schaub M, Hartmann M, Werner RA, Joseph J, Poll C, Hagedorn F (2024) Drought resistance and resilience of rhizosphere communities in forest soils from the cellular to ecosystem scale – insights from ^{13} C pulse labeling. New Phytol 242(3):960–974. https://doi.org/10.1111/nph.19612
21. Gautschi P (2017) *A new method to graphitize CO2 from atmospheric air for radiocarbon analysis* [Master thesis]. ETH Zurich
22. Graf Pannatier E, Dobbertin M, Heim A, Schmitt M, Thimonier A, Waldner P, Frey B (2012) Response of carbon fluxes to the 2003 heat wave and drought in three mature forests in Switzerland. Biogeochemistry 107(1–3):295–317. https://doi.org/10.1007/s10533-010-9554-y
23. Graven HD, Warren H, Gibbs HK, Khatiwala S, Koven C, Lester J, Levin I, Spawn-Lee SA, Wieder W (2024) Bomb radiocarbon evidence for strong global carbon uptake and turnover in terrestrial vegetation. Science 384(6702):1335–1339. https://doi.org/10.1126/science.adl4443
24. Guidi C, Frey B, Brunner I, Meusburger K, Vogel ME, Chen X, Stucky T, Gwiazdowicz DJ, Skubała P, Bose AK, Schaub M, Rigling A, Hagedorn F (2022) Soil fauna drives vertical redistribution of soil organic carbon in a long-term irrigated dry pine forest. Glob Change Biol 28(9):3145–3160. https://doi.org/10.1111/gcb.16122
25. Guidi C, Lehmann MM, Meusburger K, Saurer M, Vitali V, Peter M, Brunner I, Hagedorn F (2023) Tracing sources and turnover of soil organic matter in a long-term irrigated dry forest using a novel hydrogen isotope approach. Soil Biol Biochem 184:109113. https://doi.org/10.1016/j.soilbio.2023.109113

26. Hagedorn F, Joseph J, Peter M, Luster J, Pritsch K, Geppert U, Kerner R, Molinier V, Egli S, Schaub M, Liu J-F, Li M, Sever K, Weiler M, Siegwolf RTW, Gessler A, Arend M (2016) Recovery of trees from drought depends on belowground sink control. Nat Plants 2(8):16111. https://doi.org/10.1038/nplants.2016.111
27. Hartmann M, Brunner I, Hagedorn F, Bardgett RD, Stierli B, Herzog C, Chen X, Zingg A, Graf-Pannatier E, Rigling A, Frey B (2017) A decade of irrigation transforms the soil microbiome of a semi-arid pine forest. Mol Ecol 26(4):1190–1206. https://doi.org/10.1111/mec.13995
28. Herzog C, Steffen J, Graf Pannatier E, Hajdas I, Brunner I (2014) Nine Years of Irrigation Cause Vegetation and Fine Root Shifts in a Water-Limited Pine Forest. PLoS ONE 9(5):e96321. https://doi.org/10.1371/journal.pone.0096321
29. Hinko-Najera N, Fest B, Livesley SJ, Arndt SK (2015) Reduced throughfall decreases autotrophic respiration, but not heterotrophic respiration in a dry temperate broadleaved evergreen forest. Agric For Meteorol 200:66–77. https://doi.org/10.1016/j.agrformet.2014.09.013
30. Huang S, Ye G, Lin J, Chen K, Xu X, Ruan H, Tan F, Chen HYH (2018) Autotrophic and heterotrophic soil respiration responds asymmetrically to drought in a subtropical forest in the Southeast China. Soil Biol Biochem 123:242–249. https://doi.org/10.1016/j.soilbio.2018.04.029
31. Hunziker S, Begert M, Scherrer SC, Rigling A, Gessler A (2022) Below Average Midsummer to Early Autumn Precipitation Evolved Into the Main Driver of Sudden Scots Pine Vitality Decline in the Swiss Rhône Valley. Front Forests Global Change 5:874100. https://doi.org/10.3389/ffgc.2022.874100
32. Intergovernmental Panel On Climate Change (Ipcc) (2021) Climate Change 2021 – The Physical Science Basis: Working Group I Contribution to the Sixth Assessment Report of the Intergovernmental Panel on Climate Change, 1st edn. Cambridge University Press. https://doi.org/10.1017/9781009157896
33. Joseph J, Gao D, Backes B, Bloch C, Brunner I, Gleixner G, Haeni M, Hartmann H, Hoch G, Hug C, Kahmen A, Lehmann MM, Li M-H, Luster J, Peter M, Poll C, Rigling A, Rissanen KA, Ruehr NK, Gessler A (2020) Rhizosphere activity in an old-growth forest reacts rapidly to changes in soil moisture and shapes whole-tree carbon allocation. *Proceedings of the National Academy of Sciences*, *117*(40), 24885–24892. https://doi.org/10.1073/pnas.2014084117
34. Keith DM, Johnson EA, Valeo C (2010) Moisture cycles of the forest floor organic layer (F and H layers) during drying. Water Resour Res 46(7):2009WR007984. https://doi.org/10.1029/2009WR007984
35. Komada T, Anderson MR, Dorfmeier CL (2008) Carbonate removal from coastal sediments for the determination of organic carbon and its isotopic signatures, δ^{13}C and Δ^{14}C: Comparison of fumigation and direct acidification by hydrochloric acid. Limnol Oceanography: Methods 6(6):254–262. https://doi.org/10.4319/lom.2008.6.254
36. Kudureti A, Zhao S, Zhakyp D, Tian C (2023) Responses of soil fauna community under changing environmental conditions. J Arid Land 15(5):620–636. https://doi.org/10.1007/s40333-023-0009-4

37. Kuznetsova A, Brockhoff PB, Christensen RHB (2017) lmerTest Package: Tests in Linear Mixed Effects Models. J Stat Softw 82(13):1–26. https://doi.org/10.18637/jss.v082.i13
38. Lenth RV (2024) *Estimated Marginal means, aka Least-Squares Means*. https://CRAN.R-project.org/package=emmeans
39. Liu Y, Liu S, Wan S, Wang J, Luan J, Wang H (2016) Differential responses of soil respiration to soil warming and experimental throughfall reduction in a transitional oak forest in central China. Agric For Meteorol 226–227:186–198. https://doi.org/10.1016/j.agrformet.2016.06.003
40. Mann WB (1983) An International Reference Material for Radiocarbon Dating. Radiocarbon 25(2):519–527. https://doi.org/10.1017/S0033822200005816
41. Midwood AJ, Gebbing T, Wendler R, Sommerkorn M, Hunt JE, Millard P (2006) Collection and storage of CO_2 for ^{13}C analysis: An application to separate soil CO_2 efflux into root- and soil-derived components. Rapid Commun Mass Spectrom 20(22):3379–3384. https://doi.org/10.1002/rcm.2749
42. Minich LI, Geissbühler D, Tobler S, Udke A, Brunmayr AS, Moreno Duborgel M, McMackin C, Wacker L, Gautschi P, Haghipour N, Egli M, Kahmen A, Leifeld J, Eglinton TI, Hagedorn F (2025) *Conceptualising carbon cycling pathways across different land-use types based on rates and ages of soil-respired CO_2*. Copernicus GmbH. https://doi.org/10.5194/egusphere-2025-2267
43. Moore JW, Semmens BX (2008) Incorporating uncertainty and prior information into stable isotope mixing models. Ecol Lett 11(5):470–480. https://doi.org/10.1111/j.1461-0248.2008.01163.x
44. Muhr J, Borken W (2009) Delayed recovery of soil respiration after wetting of dry soil further reduces C losses from a Norway spruce forest soil. J Geophys Research: Biogeosciences 114(G4):2009JG000998. https://doi.org/10.1029/2009JG000998
45. Pinheiro J, Bates D, R Core Team (2025) &. *nlme: Linear and Nonlinear Mixed Effects Models* (p. 3.1–168) [Data set]. https://doi.org/10.32614/CRAN.package.nlme
46. Poorter H, Nagel O (2000) The role of biomass allocation in the growth response of plants to different levels of light, CO2, nutrients and water: A quantitative review. Australian J Plant Physiol 27(12):1191–1191. https://doi.org/10.1071/PP99173_CO
47. Ramsperger U, De Maria D, Gautschi P, Maxeiner S, Müller AM, Synal H-A, Wacker L (2024) LEA—A NOVEL LOW ENERGY ACCELERATOR FOR^{14}C DATING. Radiocarbon 66(5):1280–1288. https://doi.org/10.1017/RDC.2023.85
48. Rigling A, Bigler C, Eilmann B, Feldmeyer-Christe E, Gimmi U, Ginzler C, Graf U, Mayer P, Vacchiano G, Weber P, Wohlgemuth T, Zweifel R, Dobbertin M (2013) Driving factors of a vegetation shift from Scots pine to pubescent oak in dry Alpine forests. Glob Change Biol 19(1):229–240. https://doi.org/10.1111/gcb.12038
49. Rog I, Hilman B, Fox H, Yalin D, Qubaja R, Klein T (2024) Increased belowground tree carbon allocation in a mature mixed forest in a dry versus a wet year. Glob Change Biol 30(2):e17172. https://doi.org/10.1111/gcb.17172

50. Ruff M, Wacker L, Gäggeler HW, Suter M, Synal H-A, Szidat S (2007) A Gas Ion Source for Radiocarbon Measurements at 200 kV. Radiocarbon 49(2):307–314. https://doi.org/10.1017/S0033822200042235
51. Santonja M, Fernandez C, Proffit M, Gers C, Gauquelin T, Reiter IM, Cramer W, Baldy V (2017) Plant litter mixture partly mitigates the negative effects of extended drought on soil biota and litter decomposition in a Mediterranean oak forest. J Ecol 105(3):801–815. https://doi.org/10.1111/1365-2745.12711
52. Schimel JP (2018) Life in Dry Soils: Effects of Drought on Soil Microbial Communities and Processes. Annu Rev Ecol Evol Syst 49(1):409–432. https://doi.org/10.1146/annurev-ecolsys-110617-062614
53. Schindlbacher A, de Gonzalo C, Díaz-Pinés E, Gorría P, Matthews B, Inclán R, Zechmeister-Boltenstern S, Rubio A, Jandl R (2010) Temp Sensit For soil Org matter Decompos along two elevation gradients 115(G03018). https://doi.org/10.1029/2009JG001191
54. Schindlbacher A, Wunderlich S, Borken W, Kitzler B, Zechmeister-Boltenstern S, Jandl R (2012) Soil respiration under climate change: Prolonged summer drought offsets soil warming effects. Glob Change Biol 18(7):2270–2279. https://doi.org/10.1111/j.1365-2486.2012.02696.x
55. Schuur EAG, Trumbore SE (2006) Partitioning sources of soil respiration in boreal black spruce forest using radiocarbon. Glob Change Biol 12(2):165–176. https://doi.org/10.1111/j.1365-2486.2005.01066.x
56. Shakas A, Hediger R, Gessler A, Singha K, De Pasquale G, D'Odorico P, Wagner FM, Schaub M, Maurer H, Griess H, Gisler J, Meusburger K (2025) Does optimality partitioning theory fail for belowground traits? Insights from geophysical imaging of a drought-release experiment in a Scots Pine forest. New Phytol 245(2):546–558. https://doi.org/10.1111/nph.20245
57. Singh J, Schädler M, Demetrio W, Brown GG, Eisenhauer N (2019) Climate change effects on earthworms—A review. Soil Organisms 91(3):113–137. https://doi.org/10.25674/SO91ISS3PP114
58. Soe ARB, Buchmann N (2005) Spatial and temporal variations in soil respiration in relation to stand structure and soil parameters in an unmanaged beech forest. Tree Physiol 25(11):1427–1436. https://doi.org/10.1093/treephys/25.11.1427
59. Solly EF, Jaeger ACH, Barthel M, Werner RA, Zürcher A, Hagedorn F, Six J, Hartmann M (2023) Water limitation intensity shifts carbon allocation dynamics in Scots pine mesocosms. Plant Soil 490(1–2):499–519. https://doi.org/10.1007/s11104-023-06093-5
60. Stock BC, Jackson AL, Ward EJ, Parnell AC, Phillips DL, Semmens BX (2018) Analyzing mixing systems using a new generation of Bayesian tracer mixing models. PeerJ 6:e5096. https://doi.org/10.7717/peerj.5096
61. Synal H-A, Stocker M, Suter M (2007) MICADAS: A new compact radiocarbon AMS system. Nucl Instrum Methods Phys Res Sect B 259(1):7–13. https://doi.org/10.1016/j.nimb.2007.01.138
62. Tan B, Yin R, Zhang J, Xu Z, Liu Y, He S, Zhang L, Li H, Wang L, Liu S, You C, Peng C (2021) Temperature and Moisture Modulate the Contribution of Soil Fauna to Litter Decomposition via

Different Pathways. 24:1142–1156. https://doi.org/10.1007/s10021-020-00573-w

63. Trumbore S (2006) Carbon respired by terrestrial ecosystems – recent progress and challenges. Glob Change Biol 12(2):141–153. https://doi.org/10.1111/j.1365-2486.2006.01067.x
64. Trumbore S (2009) Radiocarbon and Soil Carbon Dynamics. Annu Rev Earth Planet Sci 37(1):47–66. https://doi.org/10.1146/annurev.earth.36.031207.124300
65. Vitali V, Schuler P, Holloway-Phillips M, D'Odorico P, Guidi C, Klesse S, Lehmann MM, Meusburger K, Schaub M, Zweifel R, Gessler A, Saurer M (2024) Finding balance: Tree-ring isotopes differentiate between acclimation and stress-induced imbalance in a long-term irrigation experiment. Glob Change Biol 30(3):e17237. https://doi.org/10.1111/gcb.17237
66. Wacker L, Christl M, Synal H-A (2010) Bats: A new tool for AMS data reduction. Nucl Instrum Methods Phys Res Sect B 268(7–8):976–979. https://doi.org/10.1016/j.nimb.2009.10.078
67. Wacker L, Němec M, Bourquin J (2010) A revolutionary graphitisation system: Fully automated, compact and simple. Nucl Instrum Methods Phys Res Sect B 268(7–8):931–934. https://doi.org/10.1016/j.nimb.2009.10.067
68. Walthert L, Graf U, Kammer A, Luster J, Pezzotta D, Zimmermann S, Hagedorn F (2010) Determination of organic and inorganic carbon, δ^{13} C, and nitrogen in soils containing carbonates after acid fumigation with HCl. J Plant Nutr Soil Sci 173(2):207–216. https://doi.org/10.1002/jpln.200900158
69. Xu X (2023) Effect of Changes in Throughfall on Soil Respiration in Global Forest Ecosystems: A Meta-Analysis. Forests 14(5):1037. https://doi.org/10.3390/f14051037
70. Zhang J, Liu S, Liu C, Wang H, Luan J, Liu X, Guo X, Niu B (2021) Different mechanisms underlying divergent responses of autotrophic and heterotrophic respiration to long-term throughfall reduction in a warm-temperate oak forest. For Ecosyst 8(1):41. https://doi.org/10.1186/s40663-021-00321-z
71. Zheng P, Wang D, Yu X, Jia G, Liu Z, Wang Y, Zhang Y (2021) Effects of drought and rainfall events on soil autotrophic respiration and heterotrophic respiration. Agric Ecosyst Environ 308:107267. https://doi.org/10.1016/j.agee.2020.107267
72. Zhou X, Zhou L, Nie Y, Fu Y, Du Z, Shao J, Zheng Z, Wang X (2016) Similar responses of soil carbon storage to drought and irrigation in terrestrial ecosystems but with contrasting mechanisms: A meta-analysis. Agric Ecosyst Environ 228:70–81. https://doi.org/10.1016/j.agee.2016.04.030
73. Zweifel R, Etzold S, Sterck F, Gessler A, Anfodillo T, Mencuccini M, Von Arx G, Lazzarin M, Haeni M, Feichtinger L, Meusburger K, Knuesel S, Walthert L, Salmon Y, Bose AK, Schoenbeck L, Hug C, De Girardi N, Giuggiola A, Rigling A (2020) Determinants of legacy effects in pine trees – implications from an irrigation-stop experiment. New Phytol 227(4):1081–1096. https://doi.org/10.1111/nph.16582

Figures

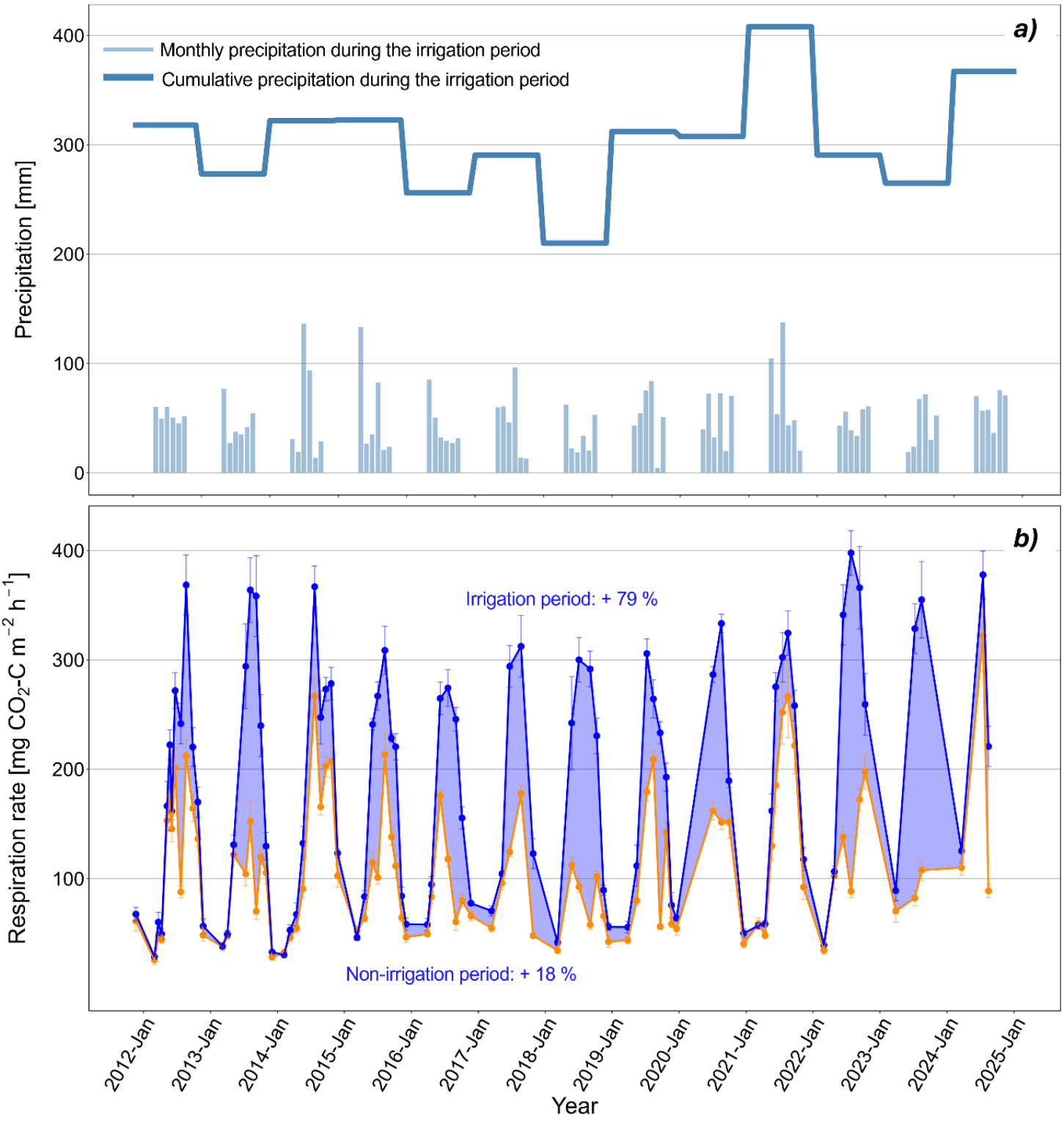


Figure 1

a) Monthly and total precipitation [mm] during the irrigation period, measured at the nearest MeteoSwiss Station in Sion from 2012 to 2024. **b)** Mean soil respiration rates (mg CO_2-C m^{-2} h^{-1}) in the dry control and irrigation treatment from winter 2012 to summer 2024. Irrigation period: May-October.

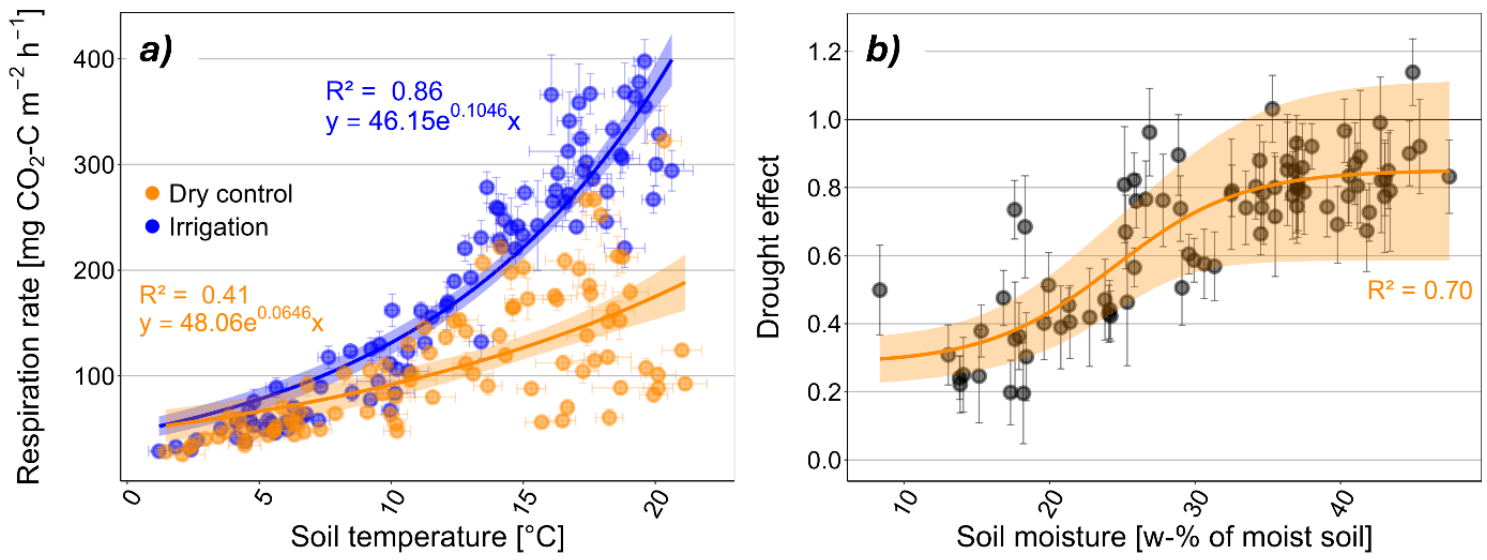


Figure 2

a) Exponential relationship between soil respiration rate (mg CO_2-C m^{-2} h^{-1}) and soil temperature (°C) in the dry control and irrigation treatment. **b)** Relationship between drought effect ($SR_{dry\ control}/SR_{irrigation}$) and soil moisture (w-% of moist soil) in the dry control treatment. The data were fitted using a Boltzmann function.

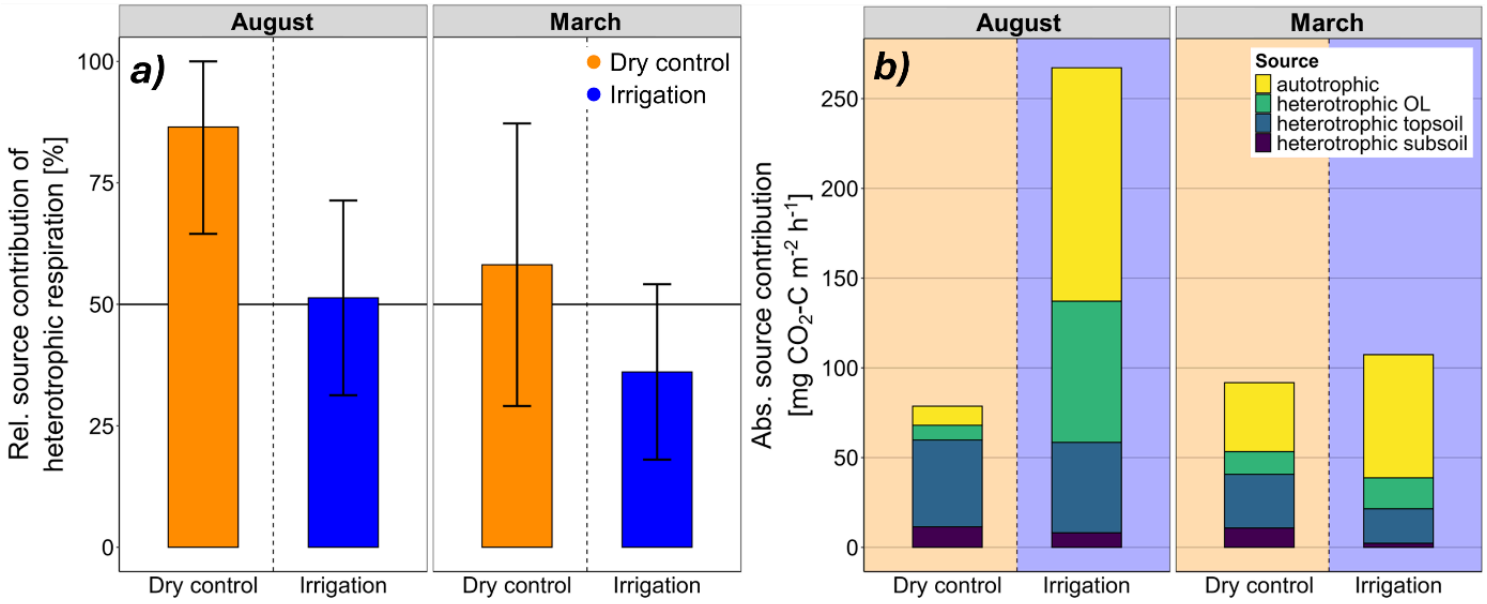


Figure 3

a): Relative contributions of heterotrophic respiration (%) in the dry control and irrigation treatments during August and March. **b):** Absolute contributions of autotrophic respiration and heterotrophic respiration (mg CO_2-C m^{-2} h^{-1}) from the organic layer (OL = Oi + Oe/Oa), topsoil (0-10 cm), and subsoil (10-20 cm) in both treatments and seasons. Mean values are shown for March. Values for replicates are presented in Figure S3.

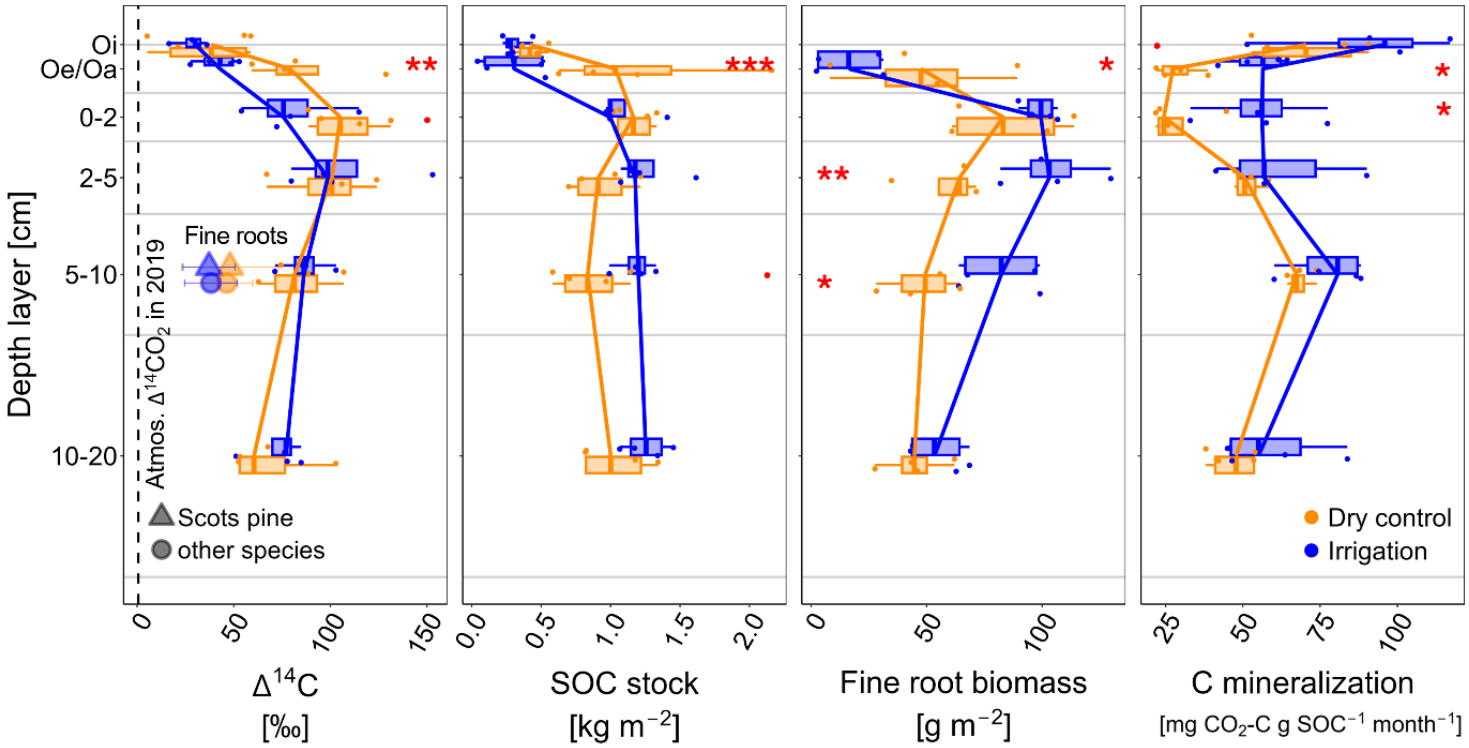


Figure 4

Boxplots of $\Delta^{14}C$ values of SOC (‰), SOC stocks (kg m^{-2}), fine root biomass (g m^{-2}), and C mineralization (mg CO_2-C g SOC^{-1} $month^{-1}$) in dry control and irrigation treatments. Also shown are mean $\Delta^{14}C$ values (‰) of fine roots from Scots pine and other species. Significant treatment differences are highlighted in red. The black dashed line indicates atmospheric $\Delta^{14}CO_2$ levels in 2019.

Supplementary Files

This is a list of supplementary files associated with this preprint. Click to download.

- image1.png
- 03manuscriptLTDpreprintsupplement.docx